JACS
JOURNAL OF THE AMERICAN CHEMICAL SOCIETY
Communication
pubs.acs.org/JACS

Cubic Box versus Spheroidal Capsule Built from Defect and Intact Pentagonal Units

Fatma Bannani,[†] Sébastien Floquet,[†] Nathalie Leclerc-Laronze,[†] Mohamed Haouas,[†] Francis Taulelle,[†] Jérôme Marrot,[†] Paul Kögerler,[‡] and Emmanuel Cadot*[,†]

[†]Institut Lavoisier de Versailles UMR 8180, Université de Versailles Saint-Quentin, 78035 Versailles, France
[‡]Institut für Anorganische Chemie, RWTH Aachen University, D-52074 Aachen, Germany

Supporting Information

ABSTRACT: The high-nuclearity polyoxothiomolybdate $[H_8Mo_{84}S_{48}O_{188}(H_2O)_{12}(CH_3COO)_{24}]^{32-}$ has been prepared and characterized by single-crystal X-ray crystallography and ^{1}H NMR, IR, Raman, and UV−vis spectroscopy. The solid-state structure reveals an unprecedented and intriguing arrangement consisting of a nanoscaled anionic cube. The surprisingly open structure of this $\{Mo_{84}\}$-type cubic box features a large inner void that is accessible via its six open square faces with diameters of ca. 9 Å. Importantly, this molecular system appears to be highly functionalizable because of the presence of 24 exposed exchangeable acetate ligands.

Polyoxometalates (POMs) are discrete polymetallic oxides that provide huge potential for the deliberate synthesis of multifunctional materials with attractive properties for a large set of applications in medicine, catalysis, and materials.[1] A remarkable feature of POM chemistry is that a few invariant archetypical building blocks are retained within structures and that the wide structural diversity and size ranges arise from the diversity of connection modes of these building units during the self-assembly process.[2] In polyoxomolybdate systems, the presence of pentagonal-type building groups allows the generation of very large clusters with nuclearities varying from 36 to 368 in discrete clusters.[3] Recently, Müller and coworkers demonstrated that the $\{Mo_2O_2S_2\}$ fragment combines with the $\{W_6O_{21}\}$ pentagonal building block to form a spherical Keplerate-type cluster composed of 12 pentagons and 30 $\{Mo_2O_2S_2\}$ linkers.[4] Herein we report that two nanosized polyoxothiomolybdates can be selectively isolated via the same synthetic procedure carried out in a concentrated acetate buffer (pH 3.6) using a Mo_2^V/Mo^{VI} ratio of 2:3. Both polyoxothiomolybdate compounds, a Keplerate and an "inverse" Keplerate, are based on $\{Mo_2O_2S_2\}$ and polyoxomolybdate fragments but differ strikingly in their constituents (i.e., the building blocks at the corners and linkers at the vertices). The Keplerate-type cluster (**2a**) exhibits the well-known spheroidal shape having approximately I_h symmetry, while the inverse Keplerate cluster (**1a**) displays an unprecedented cuboidal arrangement. Additionally, structural analyses of **1a** and **2a** provided strong evidence about the formation pathway of the pentagonal $\{Mo_6O_{21}\}$ unit, which is relevant for a better understanding of the self-assembly processes of the family of pentagon-based giant polyoxomolybdates. Both **1** and **2** were characterized by X-ray diffraction (XRD) analysis; NMR, IR, Raman, and UV−vis spectroscopies; and elemental analysis.

Compound **1** crystallized from the mother liquor as well-defined octahedral yellow crystals having the formula $Na_{43.5}(NMe_4)_{2.5}[H_{32}Mo_{84}S_{48}O_{200}(AcO)_{24}]\cdot 14AcO\cdot 140H_2O$. As depicted in Figure 1, the single-crystal XRD study of **1** revealed

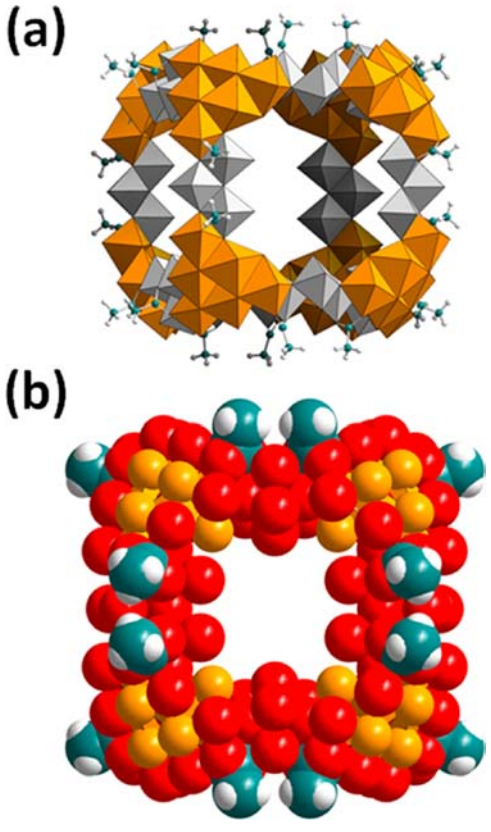

Figure 1. Representations of $[H_{32}Mo_{84}S_{48}O_{200}(AcO)_{24}]^{32-}$ (**1a**). (a) Polyhedral view highlighting the connections between the $\{Mo^{VI}{}_3O_{11}\}^{4-}$ units forming the edges (gray polyhedra) and the $\{Mo_6S_6O_6(OH)\}^{5+}$ building blocks at the corners (orange polyhedra). Acetate ligands are shown in a ball-and-stick representation. (b) Space-filling view showing one of the six large open faces (ca. 9 Å) in **1a**. O, red; S, yellow; C, blue-green; H, white.

Received: September 19, 2012
Published: November 8, 2012

   dx.doi.org/10.1021/ja309302y | J. Am. Chem. Soc. 2012, 134, 19342−19345

that the discrete anion **1a** having the formula $[H_{32}Mo_{84}S_{48}O_{200}(AcO)_{24}]^{32-}$ is arranged as a large cuboidal box. The eight corners of the cube are composed of unusual triangular oxothiohexamolybdenum units, $\{Mo_6S_6O_6(OH)\}^{5+}$ (abbreviated $\{Mo^V_6\}$), and the 12 edges are occupied by trinuclear $\{Mo_3O_{11}\}^{4-}$ oxomolybdate subunits (abbreviated $\{Mo^{VI}_3\}$); both types of units are depicted in Figure 2. Each trigonal

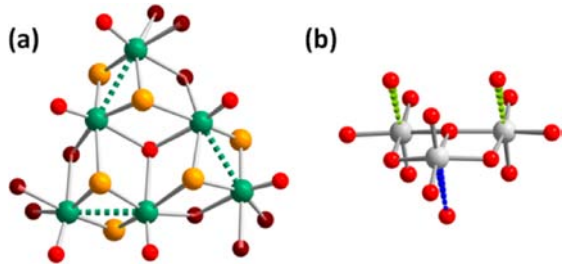

Figure 2. Ball-and-stick representations of the two constituent groups in the cuboidal structure of **1a**. (a) Structure of the trigonal $\{Mo^V_6O_6S_6(OH)\}^{5+}$ moiety showing the helicoidal disposition of the three $\{Mo_2O_2S_2\}^{2+}$ groups around the central hydroxo (C_3 axis). Color code: dotted green sticks, $Mo^V\cdots Mo^V$ bonding contacts within $\{Mo_2O_2S_2\}$ subunits; dark-red spheres, O atoms belonging to adjacent components (i.e., oxomolybdate blocks and acetate ligands). (b) Structure of the $\{Mo^{VI}_3O_{11}\}^{4-}$ linker interacting with two acetate ligands (greenish dotted lines; Mo−O = 2.28 Å) and one water molecule (blue dotted line; Mo−O = 2.55 Å).

$\{Mo^V_6\}$ unit is built from three $\{Mo_2O_2S_2\}$ fragments that are mutually connected by a central μ_3-OH group oriented trans to the three terminal O atoms belonging to {Mo═O} groups. The presence of the proton was deduced from the elongated Mo−O distance (Mo−O = 2.32 Å), yielding a bond valence sum (BVS) of 1.02 for this O atom. Furthermore, additional Mo−S contacts are observed within the $\{Mo^V_6\}$ cluster. The three inward-pointing S atoms occupy one equatorial position of neighboring Mo^V atoms, resulting in long Mo−S contacts (Mo−S = 2.58 Å), while the Mo−S bond distances in each $\{Mo_2O_2S_2\}$ subunit fall in the usual 2.29−2.36 Å range.[5] The resulting $\{Mo^V_6\}$ core has local C_3 symmetry generated by the helicoidal arrangement of the three $\{Mo_2O_2S_2\}$ fragments around the central μ_3-OH (crossed by the C_3 axis). The eight $\{Mo^V_6\}$ cationic clusters are mutually connected by 12 $\{Mo_3O_{11}\}^{4-}$ anionic fragments acting here as nearly linear linkers to generate the cuboidal arrangement. These $\{Mo^{VI}_3\}$ groups are composed of three edge-shared octahedra perpendicularly arranged around a μ_3-O atom. One additional terminal O atom attached to the central Mo^{VI} atom is assigned to a water ligand with a characteristic long Mo−OH_2 distance (Mo−OH_2 = 2.55 Å). The $\{Mo^V_6\}$ building blocks and the $\{Mo^{VI}_3\}$ linkers are connected through edge-shared junctions involving two μ_3-oxo ligands. Strikingly, 24 outward-directed acetate ligands complete the coordination sphere of the neighboring Mo^{VI} and Mo^V atoms, thus bridging the constitutive $\{Mo^V_6\}$ building block and the $\{Mo^{VI}_3\}$ linker. The helicoidal $\{Mo^V_6\}$ building blocks are chiral (C_3 symmetry), but the two enantiomers are symmetrically related by the mirror planes and are alternately located over the eight corners of the achiral cubic box (T_d symmetry). The remaining constituents (Na^+ cations, acetate anions, and water molecules) are severely disordered within the crystal lattice, and only eight sodium atoms and ca. 38 water molecules per $\{Mo_{84}\}$ were located among the 43.5 Na^+ ions and 140 crystallization water molecules expected on the basis of elemental analysis. Such a situation is frequently encountered in crystals of very large clusters such as Keplerate-type capsules.[6] Remarkably, the cuboidal arrangement exhibits six open faces with a very large diameter (ca. 9 Å), allowing free access to a huge internal volume of ca. 2100 $Å^3$. The crystal packing of **1** corresponds to a face-centered cubic (fcc) network wherein the $\{Mo_{84}\}$ clusters occupy the nodes of an fcc array [a = 41.44 Å; Figure S1 in the Supporting Information (SI)]. Such an arrangement delimits large intercluster voids comparable in dimension to those in the $\{Mo_{84}\}$ anions. These internal and external voids are occupied by the countercations (Na^+ and NMe_4^+), crystallization water, and acetate, as determined by elemental and thermogravimetric analysis.

Compound **2** was obtained as a bright-red solid and characterized by IR, Raman, and ^1H NMR spectroscopy and elemental analysis (for details, see the SI). It was identified as a salt of Keplerate-type anion[7] having the formula $(NMe_4)_{3.5}K_{3.5}Na_{38}[Mo_{132}S_{60}O_{312}(AcO)_{30}(H_2O)_{72}]\cdot 3AcO\cdot 200H_2O$; the anion, **2a**, has the formula $[Mo_{132}S_{60}O_{312}(AcO)_{30}(H_2O)_{72}]^{42-}$. Furthermore, XRD analysis confirmed unambiguously the molecular arrangement in **2a** (Figure 3). Compound **2** was

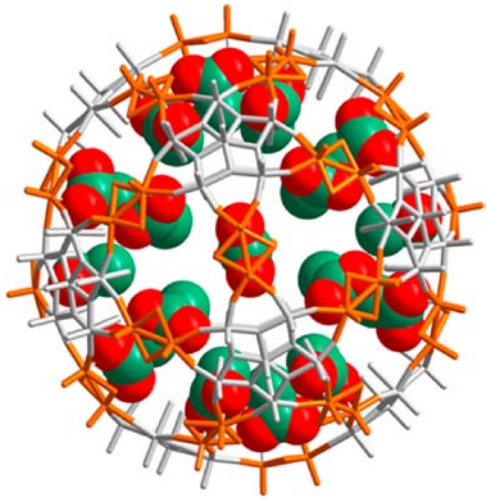

Figure 3. Mixed representation (wire and space-filling) of the sulfurated Keplerate-type anion **2a′** highlighting the 15 inner acetate ligands (green and red spheres) statistically disordered with 30 water molecules (SOF = 50%). $\{Mo_2O_2S_2\}$ linking groups are shown as orange sticks and pentagonal $\{Mo_6O_{21}(OH_2)_6\}$ building blocks as gray sticks.

recrystallized in acetate buffer to give the compound $(NMe_4)_{1.5}(NMe_2H_2)_8Na_{17.5}[Mo_{132}S_{60}O_{312}(AcO)_{15}(H_2O)_{102}]\cdot 250H_2O$ (**2′**), which contains the anion $[Mo_{132}S_{60}O_{312}(AcO)_{15}(H_2O)_{102}]^{27-}$ (**2a′**). Compounds **2** and **2′** exhibited similar spectroscopic features and differ mainly in their cationic composition and the number of acetates coordinated to the inner surface of the cluster spheres. The structure of the anion **2a′** corresponds to the well-known Keplerate-type arrangement, which has been widely described in previous studies.[7,8] The spheroidal capsule **2a′** contains the common set of 12 anionic pentagonal $\{Mo_6O_{21}(OH_2)_6\}^{6-}$ building blocks interlinked via 30 $\{Mo_2O_2S_2\}^{2+}$ cationic linkers in an icosahedral arrangement. In addition, 15 acetate ligands were found to be statistically and equally disordered [site occupancy fraction (SOF) = 50%] with 30 water molecules over the 30 $\{Mo_2O_2S_2\}$ coordination sites. The structural

dx.doi.org/10.1021/ja309302y | J. Am. Chem. Soc. 2012, 134, 19342−19345

features of the Keplerate-type anion contrast highly with those observed for **1a**, where the cationic $\{Mo_6O_6S_6(OH)\}^{5+}$ building blocks formed by three $\{Mo_2O_2S_2\}^{2+}$ units are located at the corners and the $\{Mo_3O_{11}\}^{4-}$ polyoxomolybdate fragments are located at the edges as linking groups. In addition, the acetate ligands are outward-directed in **1a** but inward-directed in **2a**. In view of all of these contrasting structural features, we call the structure of anion **1a** an "inverse" Keplerate structure.

Actually, the most interesting observation is that the inverse Keplerate (**1a**) and Keplerate (**2a**) cluster types were formed in the same reaction medium using a Mo_2^V/Mo^{VI} ratio of 2:3 at pH 3.6 at room temperature (20 °C). As soon as the reacting components, $[Mo_2O_2S_2(H_2O)_6]^{2+}$ cations and molybdate anions $[MoO_4]^{2-}$, were mixed in acetate buffer, the Keplerate cluster **2** precipitated as a bright-red solid (compound **2**). After 2 days, yellow octahedral crystals of **1** appeared. The powder XRD (PXRD) pattern of the isolated solid exhibited a fair agreement with that calculated from the X-ray structure of **1**, thus confirming its purity and homogeneity (Figure S2). Such successive events are a nice illustration of the "virtual dynamic library" of constitutional building blocks based on acidified molybdate solutions.[9] Herein, the molybdate solution produces two types of building blocks, $\{Mo_3O_{11}\}^{4-}$ and $\{Mo_6O_{21}\}^{6-}$, which are selected by the two cationic species $\{Mo_2O_2S_2\}^{2+}$ and $\{Mo_6S_6O_6(OH)\}^{5+}$, respectively. In solution, acetate ligands undoubtedly play a crucial role in stabilizing these units as labile coordination complexes that should be viewed as two latent, or virtual, components of the molybdate library (oxo and oxothio species) in solution. Furthermore, pH is also an important parameter because these latent fragments are related through simple condensation equilibria (eqs 1 and 2). Several synthesis experiments showed that in a narrow range of pH between 3.4 and 3.9, the balance between the formation of **1** and **2** was dramatically affected. According to eqs 1 and 2, as the pH is increased, the formation of **2** (Keplerate-type anion) should gradually diminish. At pH 3.9, only the formation of crystals of **1** was observed.

$$2\{Mo_3O_{11}\}^{4-} + 2H_3O^+ \rightleftarrows \{Mo_6O_{21}\}^{6-} + 3H_2O \quad (1)$$

$$\{Mo_6O_6S_6(OH)\}^{5+} + H_3O^+ \rightleftarrows 3\{Mo_2O_2S_2\}^{2+} + 2H_2O \quad (2)$$

The $\{Mo_{84}S_{48}(AcO)_{24}\}$ cubic box in anion **1a** was characterized by IR and Raman spectroscopy in the solid state and compared with the $\{Mo_{132}S_{60}(AcO)_{30}\}$ box in the Keplerate-type anion **2a** (Figure 4 and Figures S3–S5). The IR spectra of **1** and **2** show similar absorptions at ca. 1550 and 1430 cm^{-1} attributed to $\nu(CO)$ modes and related to the presence of the bridging acetato ligands.[7,10] The 1100–400 cm^{-1} range contains the main differences, related to the distinct molecular structural arrangements. The Keplerate-type compound **2** exhibits two absorptions at 792 and 851 cm^{-1} related to the two types of Mo–O–Mo bridging junctions, namely, the edge-shared junctions within pentagons and the corner-shared junctions between pentagons and $\{Mo_2O_2S_2\}$ linkers, respectively.[7] Interestingly, the IR spectrum of compound **1** shows no significant absorption in this region. Probably because of the single type of edge-shared junction in **1**, the absorptions characteristic of the bridging modes are significantly shifted to 711 and 610 cm^{-1}. Raman spectroscopy was also informative. The strong band observed at 860 cm^{-1}, which was previously assigned to the A_g vibrational breathing mode in the $\{Mo_{132}S_{60}(AcO)_{30}\}$ anion[11] (of idealized I_h symmetry), as

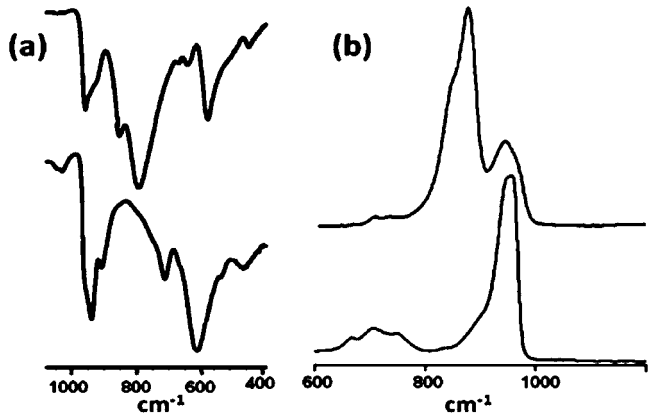

Figure 4. (a) IR and (b) Raman spectra of compounds (top) **2** and (bottom) **1** in the solid state.

expected is entirely canceled in the spectrum of **1**. Nevertheless, the $\nu_s(Mo{=}O)$ modes produce an intense resonance at 950 cm^{-1} in the spectrum of **1** and a medium band at 940 cm^{-1} in the spectrum of **2**.

Preliminary solution studies were carried out using the ^1H NMR tool box (1D, DOSY, and EXSY; see Figure 5 and

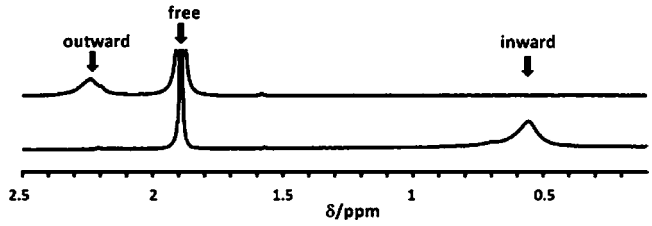

Figure 5. ^1H NMR spectra in D_2O showing the resonances of outward- (2.25 ppm) and inward-coordinated (0.55 ppm) acetates in (top) **1a** and (bottom) **2a**, respectively. Uncoordinated acetates produce the peaks at 1.9 ppm.

Figures S6 and S7). The 1D ^1H NMR spectrum of **2** in D_2O exhibits two resonances corresponding to acetates and is consistent with that previously reported for other Keplerate-type anions (Figure 5).[10] The sharp peak at 1.90 ppm is attributed to the uncoordinated acetate ligands and the broad peak at 0.55 ppm to the inner acetates coordinated at the $\{Mo_2O_2S_2\}$ linkers. Under similar conditions, compound **1** also shows two ^1H NMR resonances related to acetates, but conversely, the hydrogen nuclei of the coordinated acetate ligands appear to be significantly deshielded (2.25 ppm) with respect to those belonging to free acetates (1.90 ppm). Such a difference between the chemical shifts of the coordinated acetate ligands in **1a** and **2a** reflects their specific inner or outer locations within each compound. As usually observed, hydrogen nuclei of the methyl group are deshielded ($\Delta\delta$ = 0.35 ppm) through coordination of the acetate, while encapsulation leads to a predominant screening effect ($\Delta\delta$ = −1.35 ppm) explained by a shell effect due to the inorganic capsule. Besides, the intensity ratios of the free and coordinated acetate resonances observed in the ^1H NMR spectra of **1** and **2** do not match with those expected from the solid-state formulas. The peak of free acetates invariably remains more intense than resonance related to the coordinated acetates. Such a result is rather consistent with equilibration occurring in solution, as already evidenced for such compounds.[12] The ^1H NMR EXSY spectra of

dx.doi.org/10.1021/ja309302y | J. Am. Chem. Soc. 2012, 134, 19342–19345

compounds **1** and **2** (Figures S6c and S7c) confirmed this hypothesis by showing that ^{1}H NMR resonances corresponding to free and coordinated acetates exhibit exchange correlations, whereas the ^{1}H DOSY NMR spectra of aqueous solutions of **1** and **2** (Figures S6b and S7b) proved as expected the presence of both coordinated acetates and the corresponding free ions in solution.[13] Acetate ligands encapsulated in the Keplerate capsules **2a** (0.5 ppm) exhibit the lowest diffusion coefficient (D = 118 μm^2 s^{-1}), while the outward-oriented acetate groups in the cubic box **1a** give a higher value (D = 200 μm^2 s^{-1}). Both D values are consistent with the large sizes of molecular units **1a** and **2a**.[14] Interestingly, interactions of the NMe_4^+ ions are also nicely evidenced in the ^{1}H NMR DOSY spectra. In the presence of the Keplerate-type capsule **2a**, the NMe_4^+ ions are characterized by a deshielded chemical shift (3.42 ppm) and a relatively low diffusion coefficient (D = 187 μm^2 s^{-1}) relative to the free NMe_4^+ species (3.05 ppm and 835 μm^2 s^{-1}). When associated to the cubic box **1a**, however, NMe_4^+ ions exhibit NMR features (3.01 ppm and 783 μm^2 s^{-1}) comparable to those of the free state. This result exemplifies perfectly the host−guest properties of **2a**, where the 20 $\{Mo_9S_3O_6\}$ pores can interact with the NMe_4^+ cations. In contrast, no plausible interaction of NMe_4^+ with **1a** was detectable in relationship with the six large open faces, which preclude any specific interaction with NMe_4^+ ions.

Furthermore, the UV−vis spectra of aqueous solutions of **1** and **2** exhibit significant differences (Figures S8−S10). Compound **1** produces yellow aqueous solutions that give significant absorptions below 350 nm, identified as shoulders at 320 and 273 nm. In contrast, the UV−vis spectrum of **2** exhibits two intense maxima at 425 and 355 nm and a shoulder at 273 nm, typical for the reddish solution of the Keplerate-type anion. These absorptions correspond to E → Mo (E = O, S) ligand-to-metal charge transfer (LMCT) and herein appear to be highly sensitive to the type of junctions between the $\{Mo_2O_2S_2\}$ moieties and the oxomolybdate building blocks. These Mo^V−O−Mo^{VI} junctions are formed by μ_3-O atoms in **1** and μ_2-O atoms in **2**. Furthermore, the stabilities of compounds **1** and **2** in aqueous solution were assessed by UV−vis spectroscopy. Both appeared to be fairly stable in solution, allowing one to envisage interesting outlooks with such large assemblies.

In conclusion, we have presented a "combinatorial dynamic library" strategy involving four building blocks, namely, cationic $\{Mo_2O_2S_2\}^{2+}$ and $\{Mo_6O_6S_6OH\}^{5+}$ groups and anionic $\{Mo_3O_{11}\}^{4-}$ and $\{Mo_6O_{21}\}^{6-}$ groups, that in specific combinations lead to the formation of the sulfurated spheroidal Keplerate-type anion $\{Mo_{132}S_{60}(AcO)_{30}\}^{42-}$ or to the cuboidal inverse Keplerate-type assembly $\{Mo_{84}S_{48}(AcO)_{24}\}^{32-}$. In both cases, the underlying combinatorial processes seem to be symmetry-driven to produce high-symmetry molecular objects. Actually, the cubic box should be viewed as the first component of large POM-based molecular objects that are potentially relevant for the rational design of polyoxometalate−organic framework (POM−OF) materials through reticulation chemistry.[15] The substitution of the 24 outward-oriented acetate ligands by specific organic moieties should open the way for postfunctionalization.

■ ASSOCIATED CONTENT

Ⓢ Supporting Information

Materials, instrumentation, synthesis, crystallographic procedures and data (CIF), PXRD pattern, ^{1}H NMR spectra (1D, 2D DOSY and EXSY), vibrational spectra (IR and Raman), and UV−vis studies. This material is available free of charge via the Internet at http://pubs.acs.org.

■ AUTHOR INFORMATION

Corresponding Author

cadot@chimie.uvsq.fr

Notes

The authors declare no competing financial interest.

■ ACKNOWLEDGMENTS

The authors acknowledge the CNRS (France), the University of Versailles Saint Quentin (France), and C'nano Ile de France (Project ECOPOMs 2009) for financial support. Dr. Nathalie Guillou is acknowledged for her help with PXRD.

■ REFERENCES

(1) (a) Dolbecq, A.; Dumas, E.; Mayer, C. R.; Mialane, P. *Chem. Rev.* **2010**, *110*, 6009. (b) Long, D.-L.; Tsunashima, R.; Cronin, L. *Angew. Chem., Int. Ed.* **2010**, *49*, 1736. (c) Special issue on polyoxometalates: *Chem. Rev.* **1998**, *98*, 1−390.

(2) Pope, M. T.; Müller, A. *Angew. Chem., Int. Ed. Engl.* **1991**, *30*, 34.

(3) (a) Müller, A.; Peters, F.; Pope, M. T.; Gatteschi, D. *Chem. Rev.* **1998**, *98*, 239. (b) Müller, A.; Kögerler, P.; Dress, A. W. M. *Coord. Chem. Rev.* **2001**, *222*, 193. (c) Müller, A.; Kögerler, P.; Kuhlmann, C. *Chem. Commun.* **1999**, 1347. (d) Cronin, L.; Beugholt, C.; Krickemeyer, E.; Schmidtmann, M.; Bögge, H.; Kögerler, P.; Luong, T. K. K.; Möller, A. *Angew. Chem., Int. Ed.* **2002**, *41*, 2805.

(4) Schäffer, C.; Todea, A. M.; Bögge, H.; Cadot, E.; Gouzerh, P.; Kopilevich, S.; Weinstock, I. A.; Müller, A. *Angew. Chem.* **2011**, *123*, 12534.

(5) Marrot, J.; Pilette, M.-A.; Haouas, M.; Floquet, S.; Taulelle, F.; López, X.; Poblet, J.-M.; Cadot, E. *J. Am. Chem. Soc.* **2012**, *134*, 1724.

(6) Müller, A.; Krickmeyer, E.; Bögge, A.; Schmidtmann, M.; Roy, S.; Berkle, A. *Angew. Chem., Int. Ed.* **2002**, *41*, 3604.

(7) Müller, A.; Krickmeyer, E.; Bögge, A.; Schmidtmann, M.; Peters, F. *Angew. Chem., Int. Ed.* **1998**, *37*, 3360.

(8) (a) Müller, A.; Rehder, D.; Haupt, E. T. K.; Merca, A.; Bögge, H.; Schmidtmann, M.; Heinze-Brückner, G. *Angew. Chem., Int. Ed.* **2004**, *43*, 4466. (b) Merca, A.; Haupt, E. T. K.; Mitra, T.; Bögge, H.; Rehder, D.; Müller, A. *Chem.—Eur. J.* **2007**, *13*, 7650.

(9) Müller, A.; Kögerler, P.; Kuhlmann, C. *Chem. Commun.* **1999**, 1347.

(10) Schâffer, C.; Merca, A.; Bögge, H.; Todea, A. M.; Kistler, M. L.; Liu, T.; Thouvenot, R.; Gouzerh, P.; Müller, A. *Angew. Chem., Int. Ed.* **2009**, *48*, 149.

(11) Schäffer, C.; Todea, A. M.; Gouzerh, P.; Müller, A. *Chem. Commun.* **2012**, *48*, 350.

(12) Petina, O.; Rehder, D.; Haupt, E. T. K.; Grego, A.; Weinstock, I. A.; Merca, A.; Bögge, H.; Szakács, J.; Müller, A. *Angew. Chem., Int. Ed.* **2011**, *50*, 410.

(13) Floquet, S.; Brun, S.; Lemonnier, J.-F.; Henry, M.; Delsuc, M.-A.; Prigent, Y.; Cadot, E.; Taulelle, F. *J. Am. Chem. Soc.* **2009**, *131*, 17254.

(14) Macchioni, A.; Ciancaleoni, G.; Zuccaccia, C.; Zuccaccia, D. *Chem. Soc. Rev.* **2008**, *37*, 479.

(15) (a) Tranchemontagne, D. J.; Ni, Z.; O'Keeffe, M.; Yaghi, O. M. *Angew. Chem., Int. Ed.* **2008**, *47*, 5136. (b) Long, J. R.; Yaghi, O. M. *Chem. Soc. Rev.* **2009**, *38*, 1213.